nature portfolio

https://doi.org/10.1038/s41586-025-09611-w

Supplementary information

Wildfire smoke exposure and mortality burden in the USA under climate change

In the format provided by the authors and unedited

Supplementary Information:

Wildfire smoke exposure and mortality burden in the US under climate change

Minghao Qiu [1,2,3,4 *], Jessica Li [5], Carlos F. Gould [6], Renzhi Jing [4,7,8], Makoto Kelp [3], Marissa L. Childs [9], Jeff Wen [3], Yuanyu Xie [10], Meiyun Lin [11], Mathew V. Kiang [12], Sam Heft-Neal [5], Noah S. Diffenbaugh [3], Marshall Burke [3,5,13 *]

1 School of Marine and Atmospheric Sciences, Stony Brook University, Stony Brook, New York, USA

2 Program in Public Health, Stony Brook University, Stony Brook, New York, USA

3 Doerr School of Sustainability, Stanford University, Stanford, CA, USA

4 Center for Innovation in Global Health, Stanford University, Stanford, CA, USA

5 Center on Food Security and the Environment, Stanford University, Stanford, CA, USA

6 School of Public Health, University of California San Diego, La Jolla, CA, USA

7 Woods Institute for the Environment, Stanford University, Stanford, CA, USA

8 Department of Health Policy, School of Medicine, Stanford University, Stanford, CA, USA

9 Department of Environmental and Occupational Health Sciences, University of Washington, Seattle, WA, USA

10 School of Public Policy and International Affairs, Princeton University, Princeton, NJ, USA

11 National Oceanic and Atmospheric Administration Geophysical Fluid Dynamics Laboratory, National Oceanic and Atmospheric Administration, Princeton, NJ, USA

12 Department of Epidemiology and Population Health, School of Medicine, Stanford University, Stanford, CA, USA

13 National Bureau of Economic Research, Cambridge MA, USA

***** To whom correspondence should be addressed. E-mail: minghao.qiu@stonybrook.edu, mburke@stanford.edu

Supplementary tables

Table S1: Estimated dry matter (DM) emissions by land use type in historical period and future scenarios (unit: Million Tons, MT). For the historical period, the table shows the annual mean DM emissions from 2001-2021, derived from GFED4s. For the future scenario, the table shows the annual mean DM emissions from 2046-2055. Land use types are derived from GFED4s inventory. "Forest" includes both temperate forests and boreal forests.

Region	Type	2001 - 2021		2050 SSP3-7.0
		emissions (MT)	percent	emissions (MT)
Western US	forest	25.8	68%	145.8
	savanna	10.7	28%	102.4
	agriculture	1.7	4%	18.3
	landuse change	0.0	0%	0.0
	peatland	0.0	0%	0.0
Southeastern US	forest	4.2	28%	7.4
	savanna	5.3	35%	6.1
	agriculture	5.6	37%	5.5
	landuse change	0.0	0%	0.0
	peatland	0.0	0%	0.0
Northeastern US	forest	0.6	29%	0.7
	savanna	0.2	11%	0.4
	agriculture	1.2	60%	1.6
	landuse change	0.0	0%	0.0
	peatland	0.0	0%	0.0
Canada-Alaska	forest	152.6	94%	217.0
	savanna	0.2	0%	2.1
	agriculture	1.7	1%	6.8
	landuse change	0.0	0%	0.0
	peatland	8.2	5%	9.9
Mexico	forest	1.2	3%	1.0
	savanna	19.4	47%	34.8
	agriculture	6.4	16%	8.8
	landuse change	14.1	34%	14.7
	peatland	0.0	0%	0.0

Table S2: Performance of the selected statistical and machine learning climate-fire models. For each region, we train six algorithms {Linear, LASSO, Neural Net} $\times$ {level, log of the outcome}. The table shows the optimal spatial resolution and three evaluation metrics for each selected algorithm. The three evaluation metrics are correlation coefficient (R), bias in predicting the highest-emitting 10-year (Bias), and Root Mean Square Error divided by the mean of the outcome (RMSE/Mean). Bias is calculated as *(Prediction - Observation) / Observation* for the 10-year period with the highest emissions. Model selections are based on RMSE + |Bias| to consider both metrics. Specification denotes the three classes of climate-fire models: models that use annual average meteorological variables to predict annual fire emissions ("annual (mean)"), models that use annual average and extreme meteorological conditions to predict annual fire emissions ("annual (extreme)"), and models that use monthly average meteorological variables to predict monthly fire emissions ("monthly").

Region	**Algorithm**	**Optimal resolution**	**R**	**Bias**	**RMSE/ mean**	**Specification**
Western US	Linear, level	regional	0.98	-10%	20%	annual (mean)
	LASSO, log	regional	0.89	-3%	31%	annual (mean)
Southeastern US	Linear, level	eco3	0.51	-1%	6%	annual (mean)
	Linear, log	regional	0.76	0%	5%	annual (extreme)
	LASSO, level	regional	0.75	-1%	4%	annual (extreme)
	LASSO, log	regional	0.43	2%	6%	annual (extreme)
	Neural Net, log	regional	0.85	2%	3%	annual (extreme)
Northeastern US	Linear, level	grid	0.05	-2%	11%	annual (mean)
	Neural Net, level	eco2	0.07	2%	14%	annual (mean)
	Linear, level	regional	0.35	-2%	11%	monthly
Canada-Alaska	Linear, level	regional	0.91	4%	15%	annual (mean)
	Neural Net, log	regional	0.91	-11%	12%	annual (extreme)
Mexico	Linear, level	eco2	0.88	0%	4%	annual (mean)
	LASSO, level	eco3	0.86	0%	5%	annual (mean)
	Linear, level	grid	0.89	1%	6%	annual (extreme)
	Neural Net, log	regional	0.80	-3%	4%	monthly

Table S3: Predictive performance of the ensemble climate-fire models evaluated at different temporal scales. These metrics are calculated using out-of-sample predictions first aggregated to the regional level. Each row shows the performance of our final ensemble model across different temporal aggregations (e.g., 10-year moving average, 5-year moving average,...). The three evaluation metrics are correlation coefficient (R), bias in predicting the highest-emitting 10-year (Bias), and Root Mean Square Error over the mean of the outcome (RMSE/Mean). Bias is calculated as *(Prediction - Observation) / Observation* for the 10-year period with the highest emissions.

Region	**Temporal resolution**	**R**	**Bias**	**RMSE / Mean**
Western US	10 years	0.95	-6%	22%
	5 years	0.94	-17%	27%
	3 years	0.68	-43%	56%
	1 year	0.60	-56%	90%
Southeastern US	10 years	0.81	-1%	3%
	5 years	0.90	-8%	5%
	3 years	0.67	-22%	15%
	1 year	0.61	-30%	23%
Northeastern US	10 years	0.07	118%	120%
	5 years	-0.30	29%	129%
	3 years	-0.29	-14%	142%
	1 year	-0.03	-75%	202%
Canada-Alaska	10 years	0.92	-10%	8%
	5 years	0.81	-34%	20%
	3 years	0.57	-45%	35%
	1 year	0.09	-63%	85%
Mexico	10 years	0.87	4%	6%
	5 years	0.86	4%	9%
	3 years	0.76	-9%	13%
	1 year	0.54	-36%	37%

Table S4: Predictive performance of climate-fire models evaluated at different spatial scales. These metrics are calculated using out-of-sample predictions first aggregated to 10-year moving averages. Each row shows the performance of the model with the lowest mean square error in that region and the corresponding spatial resolution. Some models shown here are not selected in the final ensemble models. The evaluation metrics are correlation coefficient (R), and Root Mean Square Error over the mean of the outcome (RMSE/Mean).

Region	**Spatial resolution**	**R**	**RMSE/ Mean**
Western US	regional	0.98	20%
	eco3	0.88	90%
	eco2	0.82	74%
	grid	0.51	272%
Southeastern US	regional	0.88	3%
	eco3	0.77	39%
	eco2	0.43	30%
	grid	0.79	62%
Northeastern US	regional	0.51	6%
	eco3	0.41	102%
	eco2	0.57	64%
	grid	0.36	212%
Canada-Alaska	regional	0.91	12%
	eco3	0.57	160%
	eco2	0.66	91%
	grid	0.23	310%
Mexico	regional	0.80	4%
	eco3	0.88	44%
	eco2	0.83	38%
	grid	0.86	81%

Table S5: Projected smoke $PM_{2.5}$ mortality in the US under different assumptions for emissions in the Northeastern US. Given the large uncertainty in the climate-fire model in the Northeastern US, we calculate the projected mortality using the annual average fire emissions in the Northeast region from 2011-2020 ("historical emissions") and projected emissions from our climate-fire model ("projected emissions"). Emissions from other regions are from future projections. Values in the parentheses represent the 95% confidence interval estimated using 500 bootstraps.

Scenario	Projected mortality using historical emissions in NE	Projected mortality using future emissions in NE
SSP1-2.6	44714 (25247, 66335)	44776 (25172, 66451)
SSP2-4.5	46265 (25335, 69450)	46318 (25356, 69504)
SSP3-7.0	47544 (25453, 71538)	47586 (25444, 71581)

Table S6: Comparison between our fire-smoke model and similar models developed in Childs et al., 2022 (*1*) and Zhang et al., 2023 (*2*). We use temporal cross-validation to quantify the model performance of our fire-smoke model. We split the 15 years of data (2006-2020) into training and test sets by years, train our model on 14 years of data, and then evaluate model performance against the hold-out test set (1 year). The model performances of Childs et al and Zhang et al show their reported evaluation metrics on monthly data (thus comparable to the temporal resolution of our fire-smoke model). Note that our model predicts the wildfire smoke estimates generated by Childs et al. because these data provide full spatial and temporal coverage for our study period, while the other two models predict surface smoke $PM_{2.5}$ concentrations estimated at surface monitor locations.

2006-2020	**Our fire-smoke model**	**Childs et al. 2022**
RMSE (μg/m^3)	1.36	3.75
R^2	0.64	0.67
2007-2018	**Our fire-smoke model**	**Zhang et al. 2023**
RMSE (μg/m^3)	1.13	3.00
R^2	0.63	0.79

Table S7: Comparing our historical mortality estimates with prior literature. The table shows the estimated annual mortality due to smoke $PM_{2.5}$ between 2007-2020 in the contiguous US and California, respectively. The table reports results from our lag 0 and lag 0-1 models. Note that Connolly et al. only estimated smoke-related mortality in California during 2008-2018 (*3*). Estimates from Ma et al. are calculated using their reported smoke-attributable non-accidental mortality rates and population estimates used in our paper (*4*). Values in the parentheses represent 95% confidence intervals (either reported by prior papers or calculated using 500 bootstraps from our paper).

	Contiguous US			**California**		
Year	**Our paper (lag 0)**	**Our paper (lag 0-1)**	**Ma et al., 2024**	**Our paper (lag 0)**	**Our paper (lag 0-1)**	**Connolly et al., 2024**
2007	28,440 (16,894, 42,119)	43,542 (27,636, 62,695)	12,740 (7,564 - 17,916)			
2008	17,905 (10,588, 26,879)	39,875 (24,824, 57,250)	13,983 (8,509 - 19,456)	2,462 (1,194, 3,790)	4,196 (2,448, 6,300)	10,020 (890 - 18,480)
2009	12,147 (7,195, 18,225)	25,524 (15,628, 38,638)	8,028 (4,409 - 11,646)	2,021 (1,203, 3,040)	3,584 (2,013, 5,538)	2,220 (190 - 4,230)
2010	18,035 (10,614, 26,918)	27,662 (17,985, 40,662)	9,192 (5,314 - 13,070)	245 (134, 366)	1,764 (931, 2,735)	1,240 (110 - 2,370)
2011	26,452 (15,308, 39,470)	41,319 (25,557, 60,208)	13,256 (8,051 - 18,461)	361 (202, 539)	553 (327, 828)	1,500 (130 - 2,870)
2012	26,579 (15,991, 39,019)	48,375 (30,319, 69,685)	15,160 (9,499 - 20,821)	427 (235, 641)	709 (419, 1,071)	1,690 (150 - 3,230)
2013	22,116 (13,466, 32,675)	43,586 (28,069, 61,957)	13,719 (8,441 - 18,997)	1,829 (1,083, 2,732)	2,163 (1,283, 3,200)	3,400 (300 - 6,440)
2014	14,894 (8,945, 22,300)	32,143 (20,143, 46,595)	9,824 (5,668 - 13,981)	815 (473, 1,208)	2,235 (1,338, 3,423)	2,120 (180 - 4,010)
2015	21,444 (12,902, 31,835)	33,831 (22,144, 49,423)	9,802 (5,716 - 13,889)	1,131 (678, 1,666)	1,778 (1,134, 2,616)	3,480 (300 - 6,570)
2016	14,026 (8,404, 20,940)	30,732 (19,293, 44,453)	10,283 (6,075 - 14,491)	2,233 (1,322, 3,303)	3,147 (2,000, 4,598)	4,530 (400 - 8,470)
2017	22,486 (13,540, 33,624)	33,427 (20,841, 48,777)	9,354 (5,293 - 13,415)	2,494 (1,290, 3,784)	4,201 (2,468, 6,255)	12,650 (1,160 - 23,030)
2018	25,434 (14,949, 38,407)	42,444 (26,084, 62,213)	13,583 (7,802 - 19,365)	3,046 (1,344, 4,984)	4,551 (2,324, 7,186)	12,850 (1,150 - 23,730)
2019	21,159 (12,584, 31,351)	39,794 (24,621, 58,004)	13,696 (8,084 - 19,307)			
2020	28,187 (16,977, 41,509)	44,339 (28,528, 63,009)	12,999 (7,596 - 18,402)			
Period average	21,379 (13,003, 31,818)	37,614 (24,370, 54,089)	11,830 (7,001 - 16,658)	1,551 (881, 2,350)	2,626 (1,562, 3,844)	5,065 (451 - 9,400)

Table S8: Estimated annual smoke-related deaths in 2050 (SSP3-7.0 scenario) across different assumptions for future population and baseline death rate. Our main results use projected population and death rate in 2050 for the 65+ and under 65 groups, respectively. Two sensitivity analyses using historical population and/or historical death rate are shown in the table to quantify the influences of future demographic change on estimated smoke mortality. The table shows estimated results using the lag 0-1 model. Values in the parentheses represent the 95% confidence interval estimated using 500 bootstraps.

	assumptions of future population and death rate		
	future pop, future death rate	future pop, historical death rate	historical pop, historical death rate
65+	56,460 [22,670, 83,660]	48,550 [19,490, 71,950]	35,130 [14,100, 52,060]
under 65	14,960 [7,710, 19,450]	23,230 [11,970, 30,190]	22,980 [11,840, 29,860]
total	71,420 [34,930, 98,430]	71,780 [38,530, 95,550]	58,110 [32,930, 75,630]

Table S9: Comparing our future mortality estimates with prior literature. The table shows the estimated annual mortality (unit: thousands of deaths) due to fire smoke $PM_{2.5}$ under RCP4.5 scenario in 2050. Note that Ford et al., 2018 (*5*) and Park et al., 2024 (*6*) calculated the mortality for the contiguous US, while Neumann et al., 2021 (*7*) only focused on the western US. The table also shows the mortality estimated using the same health exposure-response function across different studies when possible (Krewski et al., 2009 (*8*)). Note that the estimates for the contiguous US are total annual smoke-related mortality, while the estimates for the western US are relative to the baseline period (baseline period is 2011-2020 in our paper and 1996-2005 in Neumann et al.).

Unit: thousands of death	**Contiguous U.S.**			**Western U.S.**	
	Our paper	Ford et al., 2018	Park et al., 2024	Our paper	Neumann et al., 2021
Main estimates	41.6 (lag 0) 71.2 (lag 0-1)	15 - 53	4.9 - 7.7	8.6 (lag 0) 12 (lag 0-1)	1.3
Same exposure-response function (Krewski 2009)	26.3	53		13.3	1.3

Table S10: Selected climate-fire model performance in Canada and Mexico (with and without using soil moisture as input variables).

				main model (NARR soil moisture not used)			NARR soil moisture used		
region	**algorithm**	**optimal resolution**	**specification**	**R**	**bias**	**RMSE/mean**	**R**	**bias**	**RMSE/mean**
Canada-Alaska	Linear, level	regional	annual (mean)	0.91	4%	15%	0.91	-2%	17%
Canada-Alaska	Neural Net, log	regional	annual (extreme)	0.91	-11%	12%	0.83	-17%	13%
Mexico	Linear, level	eco2	annual (mean)	0.88	0%	4%	0.87	0%	4%
Mexico	LASSO, level	eco3	annual (mean)	0.86	0%	5%	0.54	-5%	7%
Mexico	Linear, level	grid	annual (extreme)	0.89	1%	6%	0.89	0%	5%
Mexico	Neural Net, log	regional	monthly	0.80	-3%	4%	0.77	-13%	27%

Table S11: Climate models used in this study. We use projections from 28 global climate models with available output under the historical and three climate scenarios from the CMIP6 model ensembles. The spatial resolution of each model is shown in latitude × longitude (unit: degree). Resolutions are approximated for models with varying latitudes. Data is downloaded in February 2023.

Model	**Ensemble variant**	**Resolution**
ACCESS-CM2	r1i1p1f1	1.25 x 1.88
ACCESS-ESM1-5	r1i1p1f1	1.25 x 1.88
BCC-CSM2-MR	r1i1p1f1	1.12 x 1.12
CanESM5	r1i1p1f1	2.79 x 2.81
CAS-ESM2-0	r1i1p1f1	1.42 x 1.41
CESM2-WACCM	r1i1p1f1	0.94 x 1.25
CMCC-CM2-SR5	r1i1p1f1	0.94 x 1.25
CMCC-ESM2	r1i1p1f1	0.94 x 1.25
CNRM-CM6-1	r1i1p1f2	1.4 x 1.41
CNRM-CM6-1-HR	r1i1p1f2	0.5 x 0.5
CNRM-ESM2-1	r1i1p1f2	1.4 x 1.41
EC-Earth3	r1i1p1f1	0.7 x 0.7
EC-Earth3-Veg	r1i1p1f1	0.7 x 0.7
EC-Earth3-Veg-LR	r1i1p1f1	1.12 x 1.12
FGOALS-f3-L	r1i1p1f1	0.94 x 1.25
FGOALS-g3	r1i1p1f1	2.03 x 2
GFDL-ESM4	r1i1p1f1	1 x 1.25
GISS-E2-1-G	r1i1p1f2	2 x 2.5
GISS-E2-1-H	r1i1p1f2	2 x 2.5
IPSL-CM6A-LR	r1i1p1f1	1.27 x 2.5
KACE-1-0-G	r1i1p1f1	1.25 x 1.88
MIROC-ES2L	r1i1p1f2	2.79 x 2.81
MIROC6	r1i1p1f1	1.4 x 1.41
MRI-ESM2-0	r1i1p1f1	1.12 x 1.12
NorESM2-LM	r1i1p1f1	1.89 x 2.5
NorESM2-MM	r1i1p1f1	0.94 x 1.25
TaiESM1	r1i1p1f1	0.94 x 1.25
UKESM1-0-LL	r1i1p1f2	1.25 x 1.88

Supplementary figures

A

Model	Evaluation	R	RMSE/mean	Bias
Our model	LOOCV	0.95	22%	-6%
log(fire) ~ VPD	LOOCV	0.34	42%	-44%
XGBOOST grid	LOOCV	0.48	82%	-1%
XGBOOST grid	Random CV	1.00	23%	6%

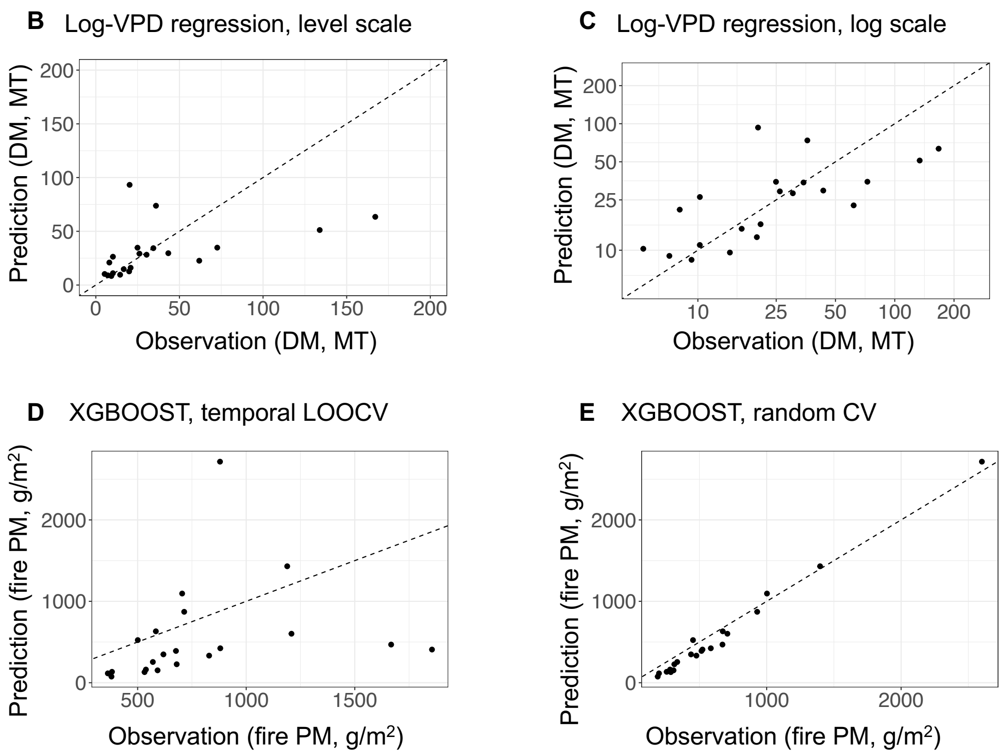

Figure S1: Predictive performance of our climate-fire model and two prior approaches. For comparison purposes, this figure only shows the results in western US. Panel A compares the predictive performance between our ensemble climate-fire model ("Our model"), a regression method that uses fire-season VPD to predict the logged fire emissions ("log(fire)-VPD") as used in (*9*), and a XGBOOST model that predicts the fire emissions at the grid cell level as used in (*10*). The table shows the correlation coefficient (R), RMSE/mean, and bias of the highest-emitting 10-year period. Panels B and C show the out-of-sample prediction from the log(fire)-VPD regressions, with the same underlying data shown in level scale (B) and log scale (C). This demonstrates that while log(fire)-VPD regression achieves reasonable performance in the log scale (as reported by previous papers), its performance is inferior to our models in predicting the absolute levels of fire emissions. Panels D and E show the out-of-sample predictions from XGBOOST model under temporal Leave-One-Out CV (LOOCV, D) and random CV (E) using the underlying dataset from (*10*). Random CV randomly partitions data to training and test sets, with the same grid cell from different years possibly existing in both training and test sets. Panels D and E suggest that the XGBOOST model trained at the grid cell has an inflated performance under random CV since grid cells can contribute data to both training and test sets.

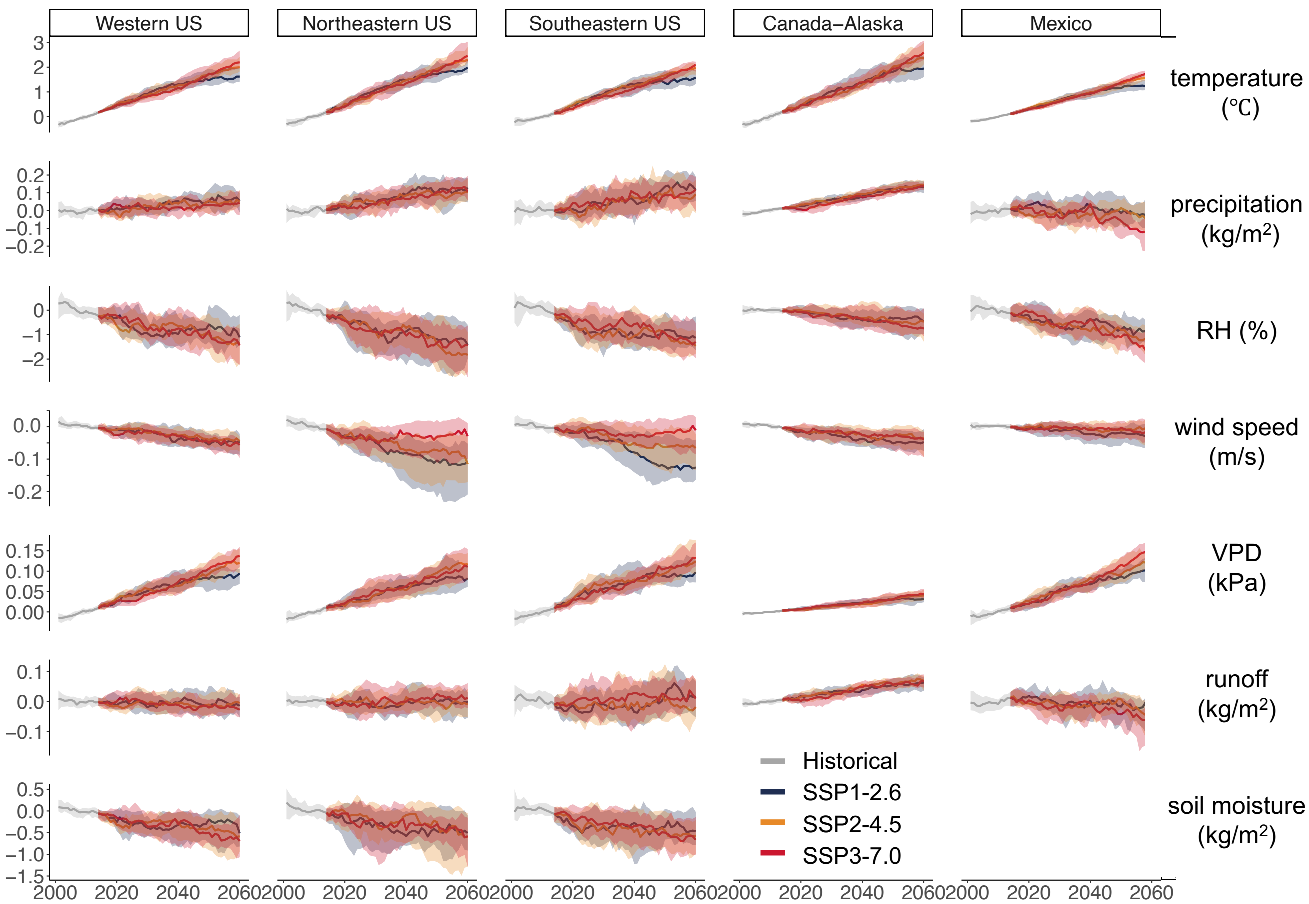

Figure S2: Projections of the climatic variables used in our climate-fire models. Color line indicates the median across 28 GCMs, and the shaded area shows the 25th and 75th percentiles across GCMs. The plot shows the 10-year moving average of the anomalies of each variable relative to the average values under historical simulations during 2001-2014. Soil moisture is not shown in Canada-Alaska and Mexico, as historical observations of soil moisture from NLDAS-2 are not available for these two regions.

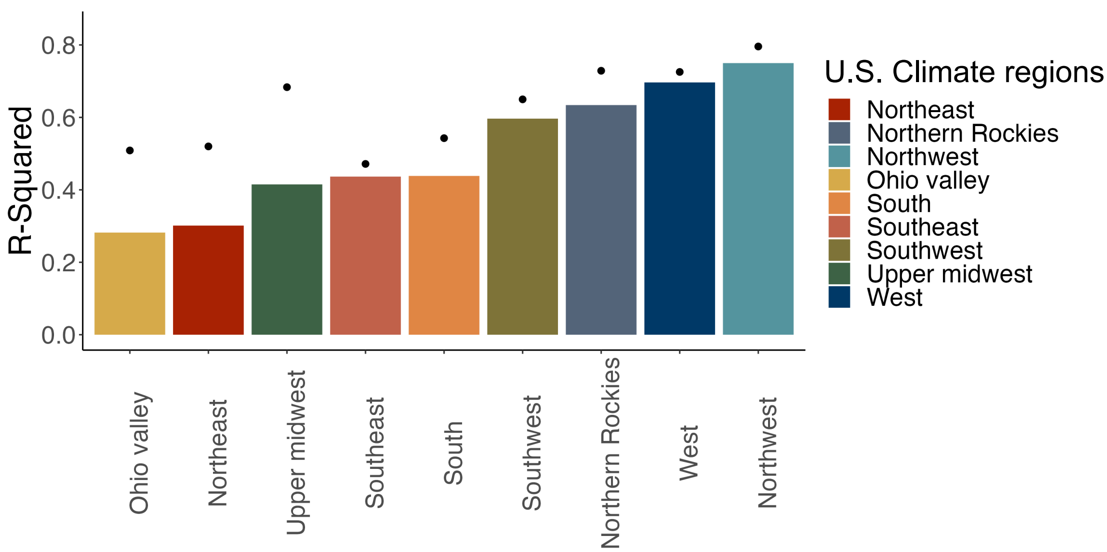

Figure S3: Performance of the fire-smoke regression models. The black dots show the full adjusted R^2 of the regression model. The color bars show the within R^2 after partialing out the month-of-year and grid cell fixed effects, quantifying the model predictive performance within each grid cell and month-of-year. Each bar shows the performance of a fire-smoke model in one of the nine US climate regions.

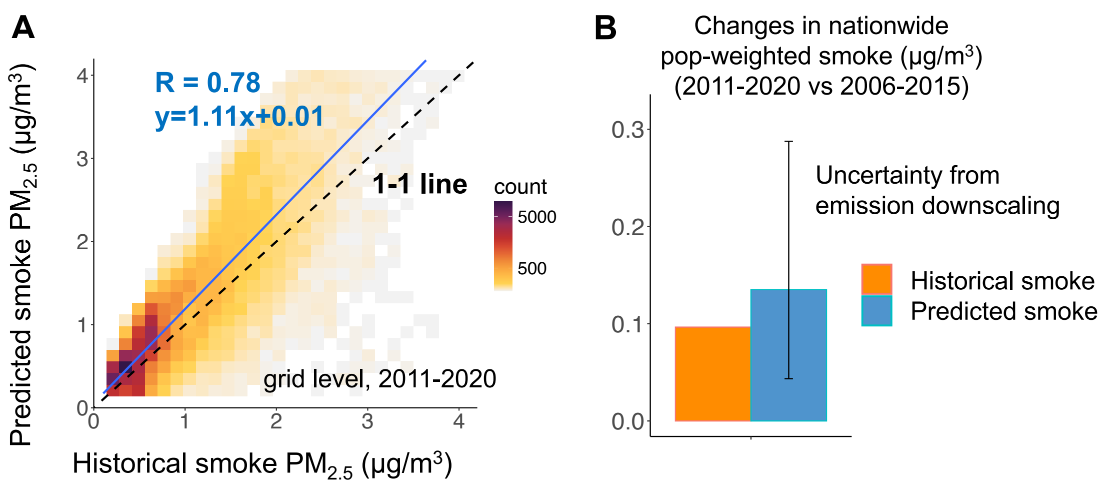

C

Smoke region	R	Pop-weighted smoke $PM_{2.5}$ (μg/m³)	
		historical	**prediction**
Northeast	0.66	0.28	0.56 [0.42, 0.70]
Northern Rockies	0.92	0.82	1.09 [0.69, 1.75]
Northwest	0.81	1.10	0.92 [0.26, 2.10]
Ohio valley	0.88	0.41	0.73 [0.42, 1.36]
South	0.94	0.49	0.43 [0.33, 0.68]
Southeast	0.07	0.29	0.29 [0.08, 0.54]
Southwest	0.87	0.35	0.46 [0.26, 1.20]
Upper midwest	0.94	0.49	0.83 [0.71, 1.06]
West	0.93	0.59	0.66 [0.49, 1.02]

Figure S4: Evaluating the entire climate-fire-smoke modeling chain against historical smoke $PM_{2.5}$ estimates. Panel A compares out-of-sample predicted smoke $PM_{2.5}$ concentrations (y-axis) with historical smoke $PM_{2.5}$ concentrations (x-axis, obtained from Childs et al. 2022). Out-of-sample predictions of smoke $PM_{2.5}$ concentrations are derived by combining out-of-sample predictions from the climate-fire model with stochastic downscaling and the fire-smoke model. The evaluations are performed at the grid level for the averaged smoke concentration over 2011-2020. Panel B shows the estimated changes in nationwide population-weighted smoke $PM_{2.5}$ between 2011-2020 and 2006-2015. The orange bar shows the results estimated using historical $PM_{2.5}$ estimates, and the blue bar shows results estimated using out-of-sample predictions of smoke $PM_{2.5}$. The blue bar shows the median value of 40 downscaling estimates, and the whiskers show the 10th and 90th percentiles. Panel C shows the evaluation results across nine smoke regions, including correlation (R) between the predicted and historical smoke, and the region-wide population-weighted smoke $PM_{2.5}$. Values in the parentheses show the range of predicted smoke due to downscaling uncertainty (n=40).

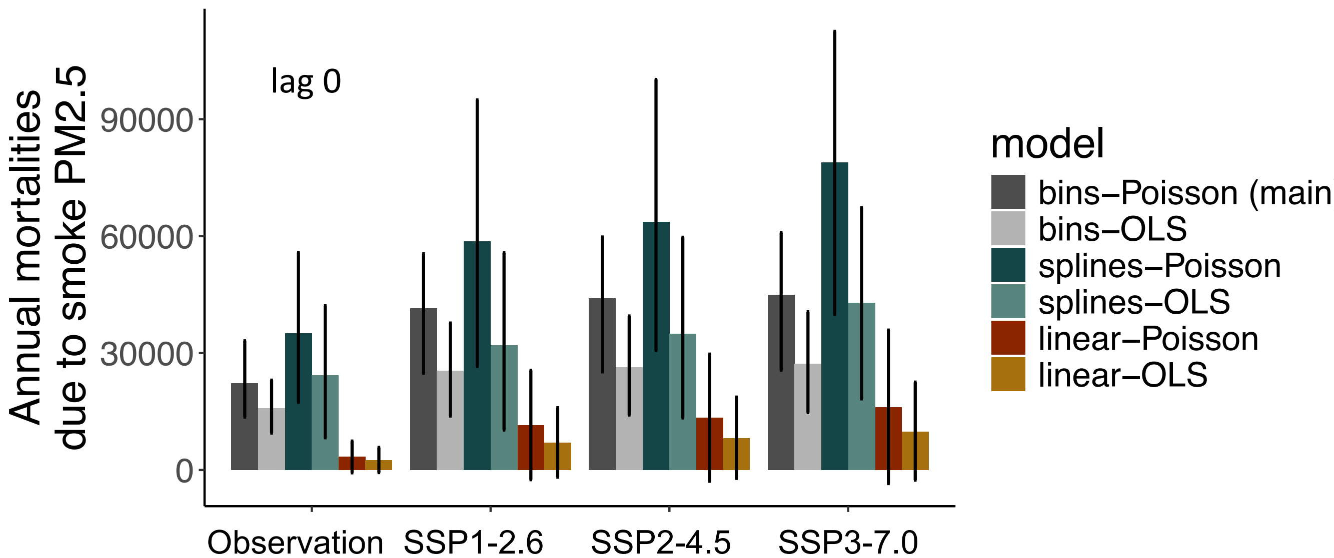

Figure S5: Estimated annual excess deaths due to smoke $PM_{2.5}$ across alternative model specifications for smoke-mortality in the historical period and future climate scenarios (2046-2055). Our main analysis uses the "bins-Poisson" specification. OLS models show results estimated using an ordinary least squares method that estimates the effects of smoke $PM_{2.5}$ on the absolute mortality rates. The bars show the mean of bootstrapped estimates, and the whiskers show the 95% bootstrapped confidence intervals (500 bootstraps). The plot shows results with lag 0 for comparison purposes.

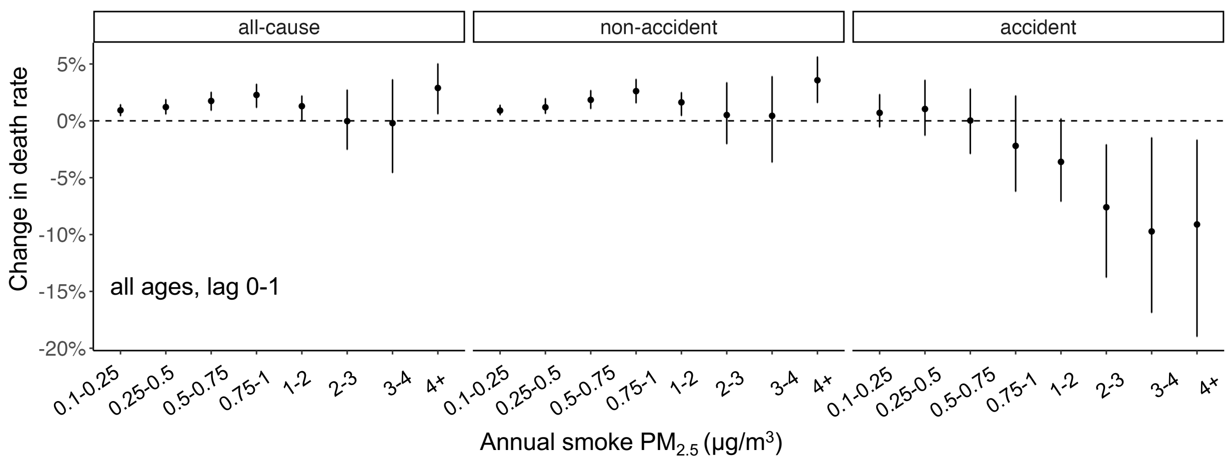

Figure S6: Empirically-estimated exposure-response function of smoke $PM_{2.5}$ on all-cause, non-accident, and accident mortality rates. Non-accidental mortality is classified with ICD-10 codes A00-R99. The figure shows the effects of exposure to different annual mean concentrations of smoke $PM_{2.5}$ (shown in annual smoke bins) relative to a year with smoke concentration $<0.1\ \mu g/m^3$. The figure reports the cumulative effects from "lag 0-1" model for the all-age group. The dots show the mean of bootstrapped estimates, and the whiskers show the 95% bootstrapped confidence intervals (500 bootstraps).

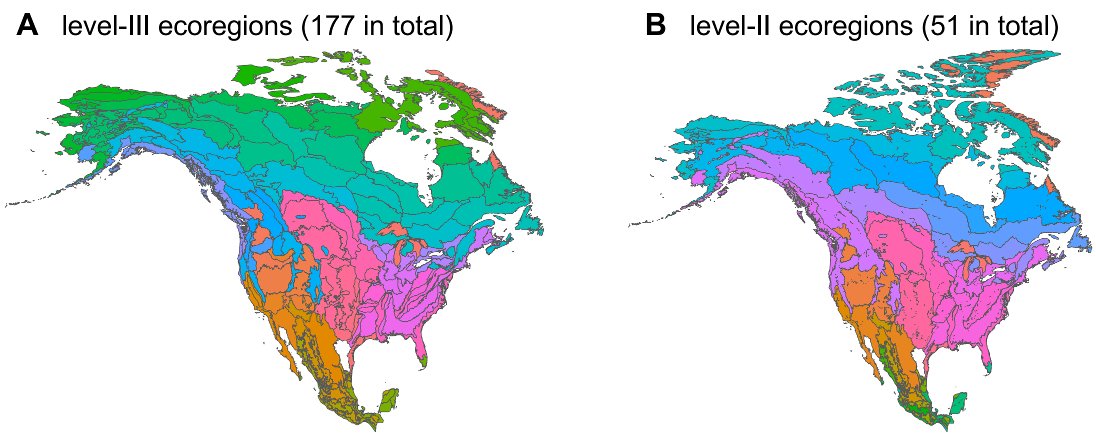

Figure S7: North America Level-3 Ecoregions (177 regions in total) and Level-2 Ecoregions (51 regions in total) considered in our model. The shape file and detailed information of the ecoregions can be found at https://www.epa.gov/eco-research/ecoregions-north-america.

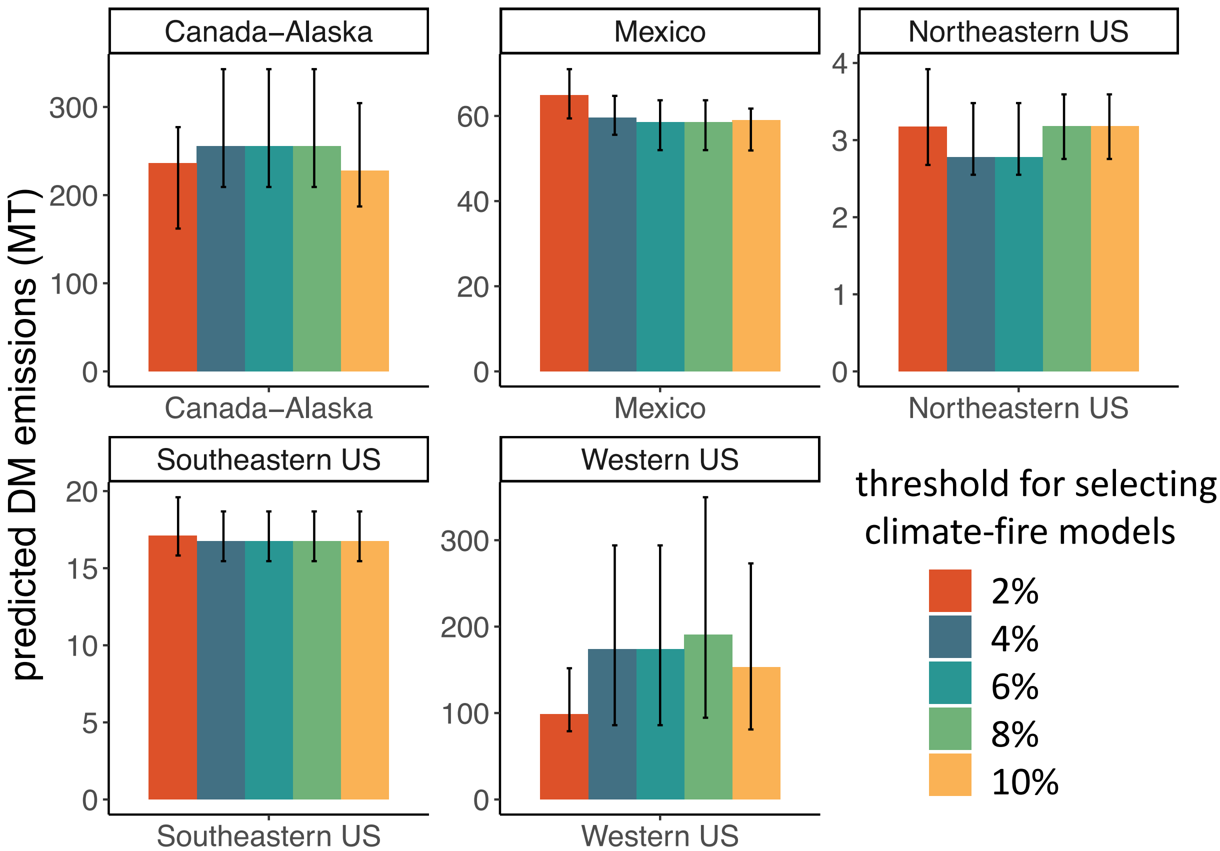

Figure S8: Projected wildfire dry matter emissions (unit: Million Tons, MT) across different thresholds for selecting ensemble climate-fire models. The plot shows the 10-year moving average of wildfire emission projections (median across GCMs) from 2046-2055. The error bar represents the 25th and 75th percentiles of the projected emissions across the 28 GCMs. The colors show results from ensemble models selected under different threshold values, i.e. the maximum deviation from the best model. In our main analysis, we select all models whose RMSE/mean + |Bias| are within 4% of the best model for each region (i.e. threshold = 4%).

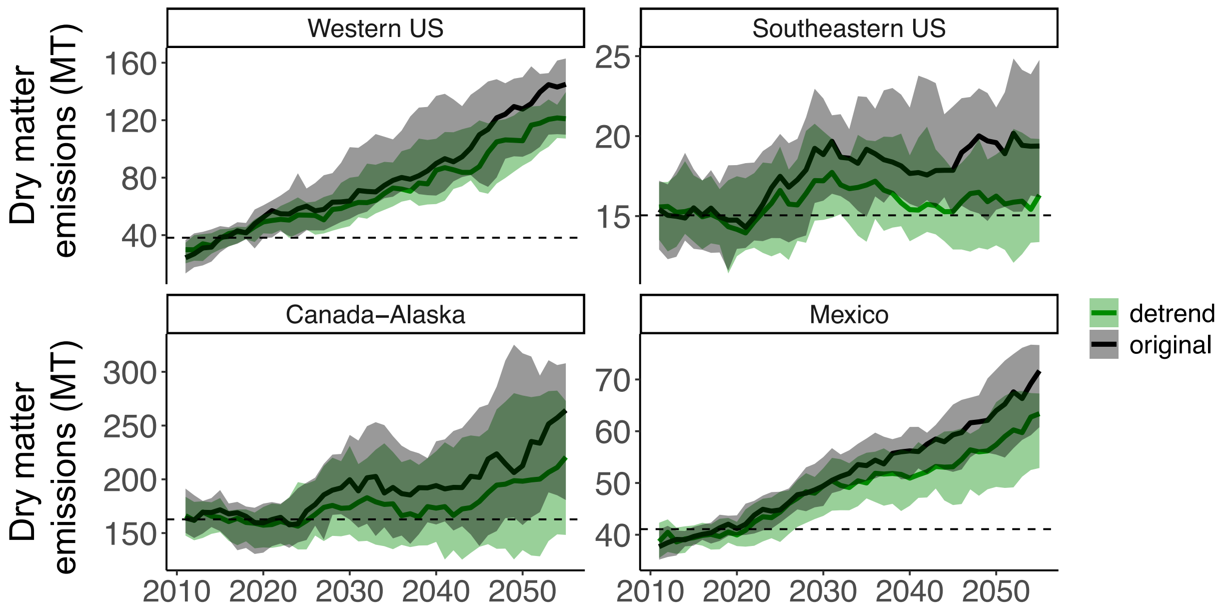

Figure S9: Projected wildfire dry matter emissions (unit: Million Tons, MT) under the historical scenario and SSP3-7.0 scenario by selected linear models. The plot shows the 10-year moving average of wildfire emission projections (median across 28 GCMs). The black lines show the emissions projected using original linear models (which are selected in our ensemble climate-fire models). The green lines show the emissions projected using the same linear models trained with detrended data (i.e. we first remove linear trends in the outcome and meteorological variables). The dashed line represents average emissions over 2001-2021 for each region. The shaded area represents the 25th and 75th percentiles of the projected emissions across the 28 GCMs.

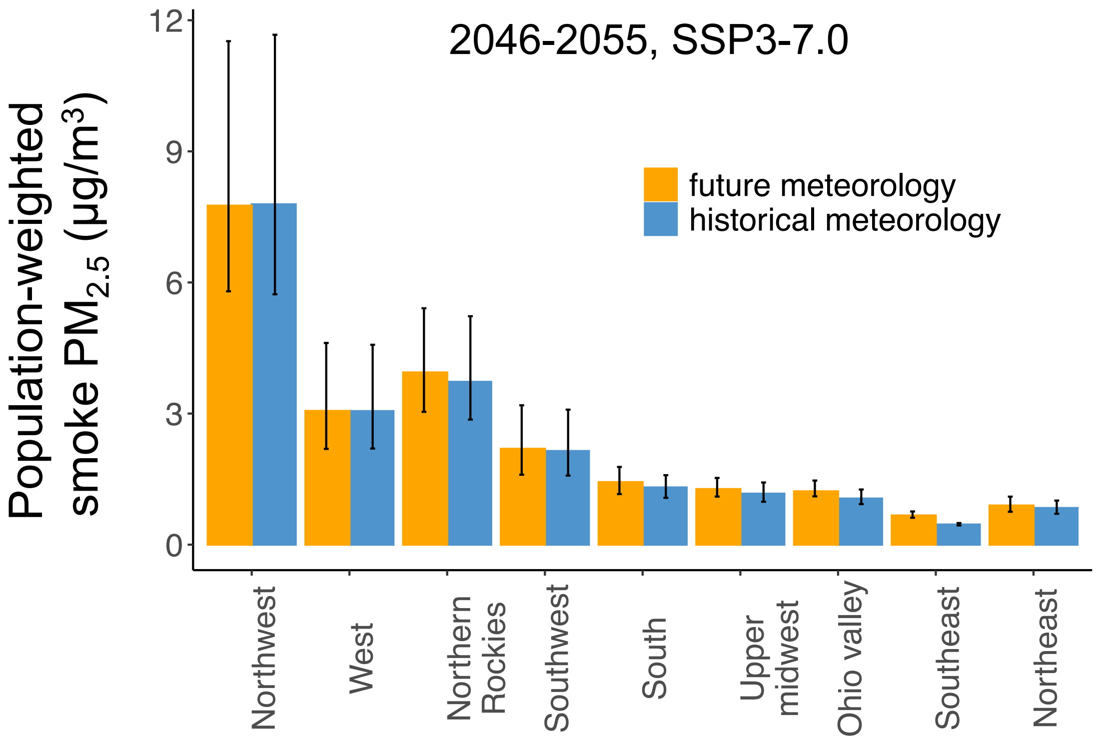

Figure S10: Population-weighted smoke $PM_{2.5}$ concentrations estimated using historical and future meteorological conditions (surface temperature, precipitation, relative humidity, and wind speed). Smoke $PM_{2.5}$ concentration is estimated using the same projected fire emissions but different meteorological conditions. The blue bars show our main estimate calculated using the historical meteorological conditions (monthly average during 2006-2020 from gridMET). The orange bars show estimated smoke $PM_{2.5}$ concentrations using future meteorological conditions (monthly average during 2046-2055, derived from 28 CMIP6 climate models). The bars show the median of 28 GCMs, and the whiskers represent the 25th and 75th percentiles across 28 climate models.

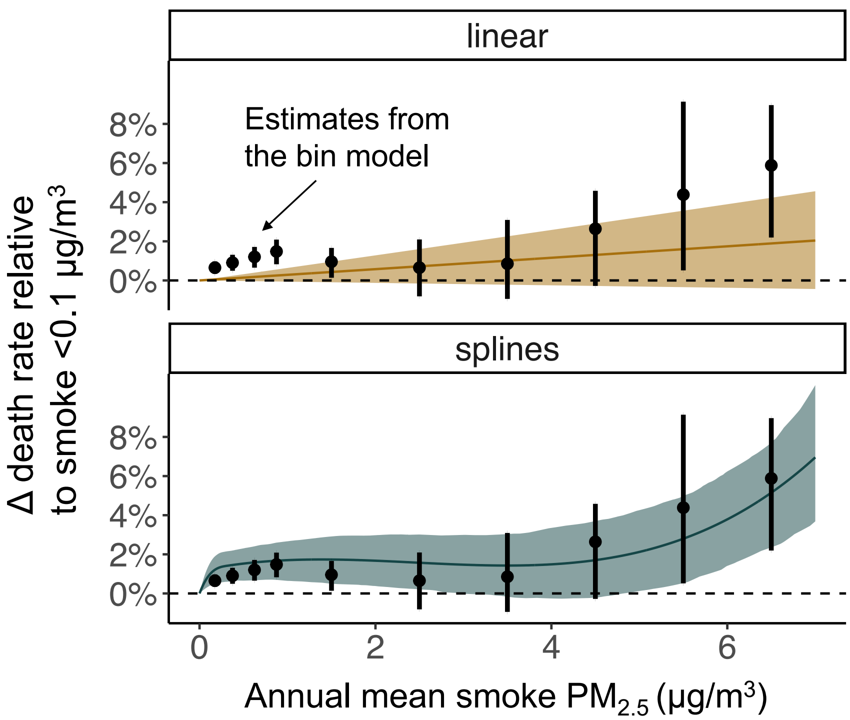

Figure S11: Impacts of smoke $PM_{2.5}$ concentration on mortality rates estimated using two alternative exposure-response functions. The two color lines show the estimated results from a linear and a spline model. All models are estimated using Poisson regressions. For comparison, the black dots show the estimated coefficients from our main model (bin model). The shaded areas and error bars represent the 95% confidence interval estimated using bootstrap procedure (500 bootstraps). Note here we use lag 0 and finer smoke bins for comparison purposes.

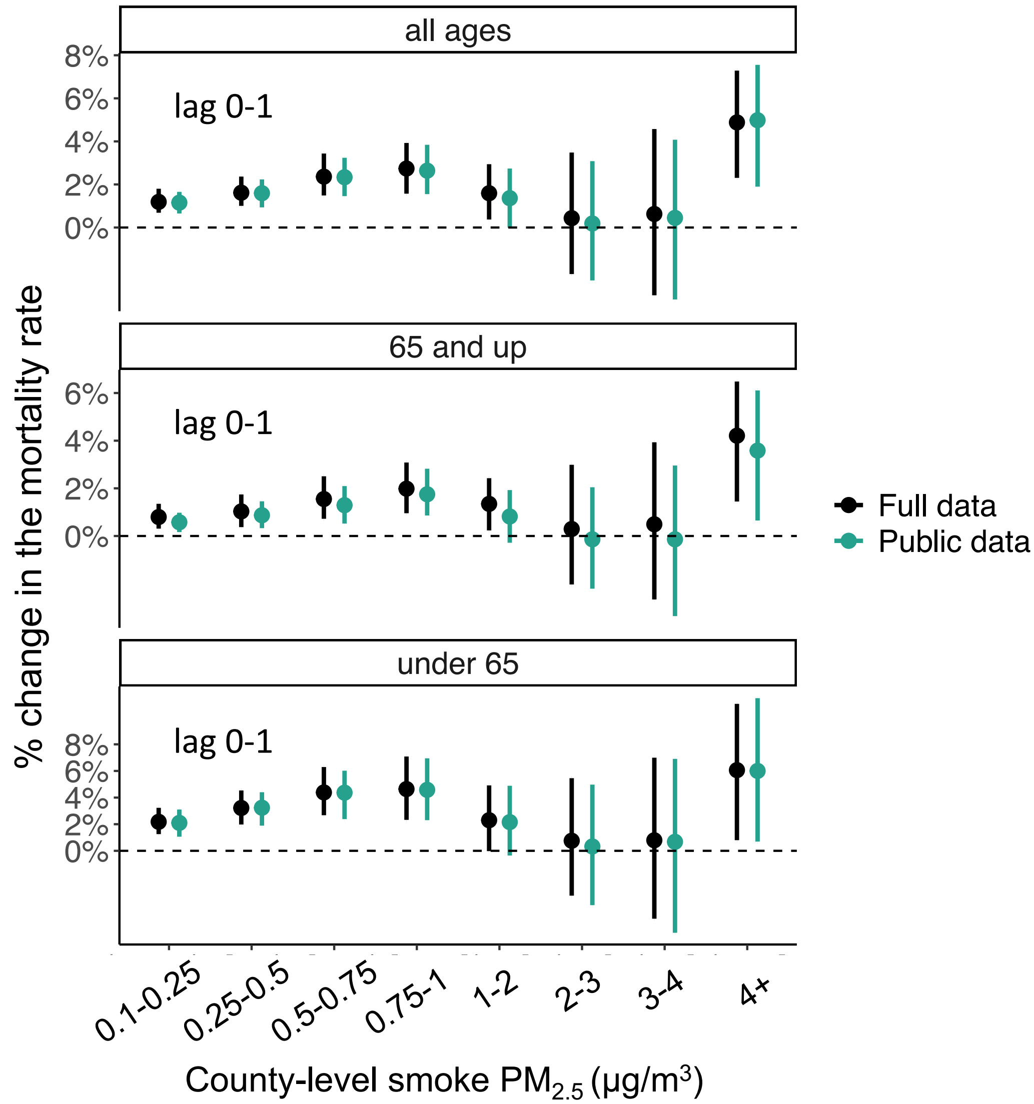

Figure S12: Empirically estimated exposure-response function of smoke $PM_{2.5}$ on mortality rate using full (restricted) data used in our analysis and public mortality data derived from CDC WONDER. Dots show the mean of the bootstrapped estimates, and whiskers show 95% confidence intervals (500 bootstraps). While we cannot share the full mortality data we used for the analysis as requested by the National Center for Health Statistics, we publicly release a dataset based on the public mortality data (derived from the CDC WONDER) in our data repository. The public data include 2374 counties with complete data in all years for all age groups, and additional counties with data in some years, as compared to the full data which cover 3077 counties in every year. We find that the estimated exposure-response function between smoke and mortality remains highly similar when using the public mortality data.

References

1. M. L. Childs *et al.*, Daily Local-Level Estimates of Ambient Wildfire Smoke PM2. 5 for the Contiguous US. *Environmental Science & Technology* **56**, 13607–13621 (2022).
2. D. Zhang *et al.*, Wildland Fires Worsened Population Exposure to PM2. 5 Pollution in the Contiguous United States. *Environmental Science & Technology* **57**, 19990–19998 (2023).
3. R. Connolly *et al.*, Mortality attributable to PM2.5 from wildland fires in California from 2008 to 2018. *Science Advances* **10**, eadl1252 (2024).
4. Y. Ma *et al.*, Long-term exposure to wildland fire smoke PM2. 5 and mortality in the contiguous United States. *Proceedings of the National Academy of Sciences* **121**, e2403960121 (2024).
5. B. Ford *et al.*, Future fire impacts on smoke concentrations, visibility, and health in the contiguous United States. *GeoHealth* **2**, 229–247 (2018).
6. C. Y. Park *et al.*, Future fire-PM2. 5 mortality varies depending on climate and socioeconomic changes. *Environmental Research Letters* **19**, 024003 (2024).
7. J. E. Neumann *et al.*, Estimating PM2. 5-related premature mortality and morbidity associated with future wildfire emissions in the western US. *Environmental Research Letters* **16**, 035019 (2021).
8. D. Krewski *et al.*, Extended follow-up and spatial analysis of the American Cancer Society study linking particulate air pollution and mortality. *Research report (Health Effects Institute)*, ISSN: 10415505 (2009).
9. J. T. Abatzoglou, A. P. Williams, Impact of anthropogenic climate change on wildfire across western US forests. *Proceedings of the National Academy of Sciences* **113**, 11770–11775 (2016).
10. S. S.-C. Wang, Y. Qian, L. R. Leung, Y. Zhang, Interpreting machine learning prediction of fire emissions and comparison with FireMIP process-based models. *Atmospheric Chemistry and Physics* **22**, 3445–3468 (2022).